Biomedical engineering

Pointwise Hölder exponents of a model for skin laser Doppler flowmetry signals based on six nonlinear coupled oscillators with linear and parametric couplings: Comparison with experimental data from young healthy subjects

Exposants de Hölder ponctuels d'une modélisation de signaux laser Doppler basée sur six oscillateurs couplés non linéaires avec des couplages linéaires et paramétriques : comparaison avec des données expérimentales provenant de sujets sains jeunes

B. Buard [a,*,b], A. Humeau [a,b], D. Rousseau [b], F. Chapeau-Blondeau [b], P. Abraham [c]

[a] *Groupe ESAIP, 18, rue du 8-Mai-1945, BP 80022, 49180 Saint-Barthélémy-d'Anjou cedex, France*
[b] *Laboratoire d'ingénierie des systèmes automatisés (LISA), université d'Angers, 62, avenue Notre-Dame-du-Lac, 49000 Angers, France*
[c] *Laboratoire de physiologie et d'explorations vasculaires, UMR CNRS 6214–Inserm 771, centre hospitalier universitaire d'Angers, 49033 Angers cedex 01, France*

Abstract

We study pointwise Hölder exponents of experimental and numerically simulated skin laser Doppler flowmetry (LDF) data that give a peripheral view of the cardiovascular system. The experimental signals are recorded in the forearm of young healthy subjects. The numerically simulated LDF data are computed from a model containing six nonlinear coupled oscillators reflecting six almost periodic rhythmic activities present in experimental LDF signals. Simulated LDF signals are for the first time generated with both linear and parametric couplings in order to represent cardiovascular system behaviors. Moreover, we propose the use of a parametric generalised quadratic variation (GQV) based estimation method for the estimation of the pointwise Hölder exponents. The latter identify possible multifractal characteristics of data. The GQV method is first tested on a white noise measure and then applied on the LDF data. The results of our signal processing analysis show that experimental LDF signals recorded in the forearm are weakly multifractal for young healthy subjects at rest. Furthermore, our findings show that the simulated data have a complexity similar to the one of signal recorded in young healthy subjects. However, their pointwise Hölder exponents have differences that we explain. This paper provides useful information to go deeper into the modeling of LDF data, which could bring enlightenment for a better understanding of the peripheral cardiovascular system.
© 2009 Elsevier Masson SAS. All rights reserved.

Keywords: Biomedical engineering; Hölder exponent; Laser Doppler flowmetry; Multifractality; Nonlinear oscillator

Résumé

Nous analysons dans cet article la complexité des signaux laser Doppler qui donnent une vue périphérique du système cardiovasculaire. Pour cela, des signaux laser Doppler expérimentaux et simulés numériquement sont étudiés. Les signaux expérimentaux sont enregistrés sur l'avant-bras de sujets sains jeunes. Les données simulées sont générées à partir d'un modèle contenant six oscillateurs non linéaires couplés reflétant six activités quasi périodiques présentes dans les signaux expérimentaux. Dans le modèle, les oscillateurs sont couplés avec deux types de couplages, linéaires et paramétriques, afin de représenter au mieux le comportement du système cardiovasculaire. À notre connaissance, de tels signaux n'ont encore jamais été présentés. La complexité de tous les signaux (expérimentaux et simulés) est étudiée par l'estimation des exposants ponctuels de Hölder. Ces derniers identifient des caractéristiques multifractales des données. Les exposants ponctuels de Hölder sont estimés à l'aide d'une méthode basée sur une variation quadratique généralisée paramétrée, préalablement testée sur une mesure de bruit blanc. Les résultats de notre analyse montrent que les signaux laser Doppler expérimentaux enregistrés sur l'avant-bras sont faiblement multifractals pour des sujets

* Corresponding author.
E-mail address: bbuard@esaip.org (B. Buard).

sains jeunes au repos. En outre, nos constatations montrent que les données simulées reflètent une complexité similaire à celle des signaux obtenus sur des sujets sains jeunes. Leurs exposants ponctuels de Hölder ont, cependant, des différences que nous explicitons. Cet article fournit des informations utiles pour aller plus loin dans la modélisation des données laser Doppler, ce qui pourrait apporter des éclaircissements pour une meilleure compréhension du système cardiovasculaire périphérique.

1. Introduction

Laser Doppler flowmetry (LDF) is commonly used in clinical research for monitoring microvascular perfusion. LDF signals are generated by the interaction between photons of a laser light and moving scatterers, mainly red blood cells. Both concentration and velocity of the moving scatterers affect the LDF perfusion estimate [1].

In this paper, we propose to analyze and compare the complexity of experimental and numerically simulated LDF signals, which give a peripheral view of the cardiovascular system. The experimental signals are recorded in the forearm of young healthy subjects. A recent work has led to the conclusion that LDF signals recorded in the forearm of young healthy subjects at rest are weakly multifractal [2]. However, it has also been shown that the ageing can reduce complexity of LDF signals [3]. This information is important as it could help in the modeling of the peripheral cardiovascular system: an accurate modeling should behave in the same way as the system it aims to reproduce. In order to simulate LDF signals, a set of five nonlinear oscillators coupled with linear couplings has recently been proposed as a theoretical model [4–6]. We propose herein to numerically simulate, for the first time, LDF signals with *six* nonlinear oscillators (reflecting six almost periodic rhythmic activities present in experimental LDF signals). Moreover, we propose to use a combination of *both* linear and parametric couplings (in order to represent cardiovascular system behaviors [6]). To analyze the multifractality of these simulated signals, an estimation of their pointwise Hölder exponents is done in comparison with the ones of experimental LDF signals. For the estimation of the Hölder exponents, we use the parametric generalised quadratic variation (GQV) based estimation method as the latter, being applied on microvascular data, has proved to give interesting results [2,4]. Moreover, in order to have a better interpretation of the results, the GQV based estimation method is first used on a measure of white noise and on a fractional Brownian motion (fBm).

Our paper is organized as follows: we first introduce the theoretical model of LDF signals. Then, the theory of the GQV method is presented and applied on a white noise measure. We then apply the GQV method on simulated, experimental LDF data and fBm and present the results that we comment. Finally, we end with a conclusion.

2. Theoretical model of laser Doppler flowmetry signals

2.1. Physiological and theoretical principles

On the time scale of minutes, six subsystems can be considered to contribute to the regulation of blood flow. Thus, under stationary conditions, when a healthy subject is at physical and mental pause, six characteristic frequencies can be found in LDF signals [7,8]:

- 1.1 Hz for the heartbeats;
- 0.36 Hz for the respiration;
- 0.1 Hz for the myogenic activity;
- 0.04 Hz for the neurogenic activity;
- 0.01 Hz for the endothelial-related metabolic activity;
- 0.007 Hz for endothelium mechanisms, such as endothelium-derived hyperpolarizing factor (EDHF).

The last one has recently been found [8]. The characteristic frequency values are different from subject to subject, but are found in the same frequency intervals for all subjects [9].

As a result of mutual couplings between the subsystems, Ref. [4] has shown that the values of the characteristic frequencies are time-variable and that their corresponding amplitudes are modulated. Based on these findings, some authors proposed to simulate LDF signals with five nonlinear coupled oscillators [4–6]. To take into account the recent results [8], a sixth oscillator has been added in our simulation. The same type of oscillator is used for all six subsystems. Due to the fact that oscillators are robust (characteristic frequencies are found in different part of the systems), and nonlinear (synchronization phenomena are observed), the basic unit in the model is written as the Poincaré oscillator [4–6]:

$$\dot{x}_i = -x_i q_i - \omega_i y_i \tag{1}$$

$$\dot{y}_i = -y_i q_i + \omega_i x_i \tag{2}$$

with $q_i = \left(\sqrt{x_i^2 + y_i^2} - a_i \right) \times \alpha_i$ where x and y are vectors of oscillators state variables. The first one (x) describes the blood flow generated by the oscillator, and the second one (y) is used for the flow velocity contribution of the oscillator. The index i denotes the ith oscillator:

- $i = 1$ for the cardiac activity;
- $i = 2$ for the respiratory activity;
- $i = 3$ for the myogenic activity;
- $i = 4$ for the neurogenic activity;
- $i = 5$ for the endothelial-related metabolic activity;
- $i = 6$ for the endothelium mechanisms, such as EDHF.

The constant α_i determines the stability, a_i is the amplitude and ω_i is the characteristic angular frequency of the oscillator. This is not the only possibility but one of the simplest. Since we have to deal with six nonlinear oscillators, it is important to

choose a basic oscillator as simple as possible. Introducing the mutual impact of the subsystems as couplings, the equations of the oscillators are modified into:

$$\dot{x}_i = -x_i q_i - \omega_i y_i + g_{x_i}(x) \tag{3}$$

$$\dot{y}_i = -y_i q_i + \omega_i x_i + g_{y_i}(y) \tag{4}$$

where $g_{x_i}(x)$ and $g_{y_i}(y)$ are coupling vectors. It has been suggested that both linear and parametric couplings have to be taken into account [6]. That is why, for the first time, mixed couplings (linear and parametric) are introduced herein in the simulated signals.

For the rhythmic cardiac activity the model is then:

$$\dot{x}_1 = -x_1 q_1 + \eta_2 x_2 - \eta_3 x_3 - \eta_4 x_4 + \eta_5 x_5 + \eta_6 x_6$$
$$- y_1(\omega_1 + \eta_2 x_2 - \eta_3 x_3 - \eta_4 x_4 + \eta_5 x_5 + \eta_6 x_6) \tag{5}$$

where η_i denotes the coupling terms, i.e. the influence of the *ith* oscillator on the cardiac activity. Modulation phenomena can be observed between respiratory and cardiac activity. For example the amplitude of the flow component resulting from the heartbeat in the peripheral blood flow is modulated by the respiration frequency. That is why a positive influence of the respiratory (η_2) is considered. The increased activity of the myogenic and neurogenic systems results in a decrease of the cardiac activity, thus negative coupling terms ($-\eta_3$ et $-\eta_4$) are chosen. Increased metabolic activity results in an increased heart rate: a positive control loop is therefore assigned to this activity (η_5 and η_6). A similar equation is used for $\dot{y}_1$. Moreover, adding noise in equation (5) generate epochs of synchronization in the cardiorespiratory synchrograms as those observed in healthy subjects. Without this random term, only the standard regimes of phase-locking, phase modulation and their interplay can be observed [6]. Based on Ref. [6], the five other subsystems in the model are in the same form.

2.2. Adjustment of the model

In the present work, the above-mentioned model is numerically simulated. For this purpose, we sum the different blood flow values ($\dot{x}_i$) and weight the sum by coefficients. The adjustment (choice of the weight coefficients) is done from the frequency domain: the constant parameters of the model are chosen so that the power spectrum of the simulated signal is close to the power spectrum of experimental LDF signals. Experimental signals have been recorded on seven young healthy men (between 20 and 36 years) with a laser Doppler flowmeter (Periflux 5000, Perimed AB, Stockholm, Sweden) and a probe positioned on the forearm. The frequency sample of these signals is 20 Hz and 20,000 points have been analyzed. An experimental and the simulated LDF signal are shown in Fig. 1. The corresponding representations in the frequency domain are shown in Fig. 2.
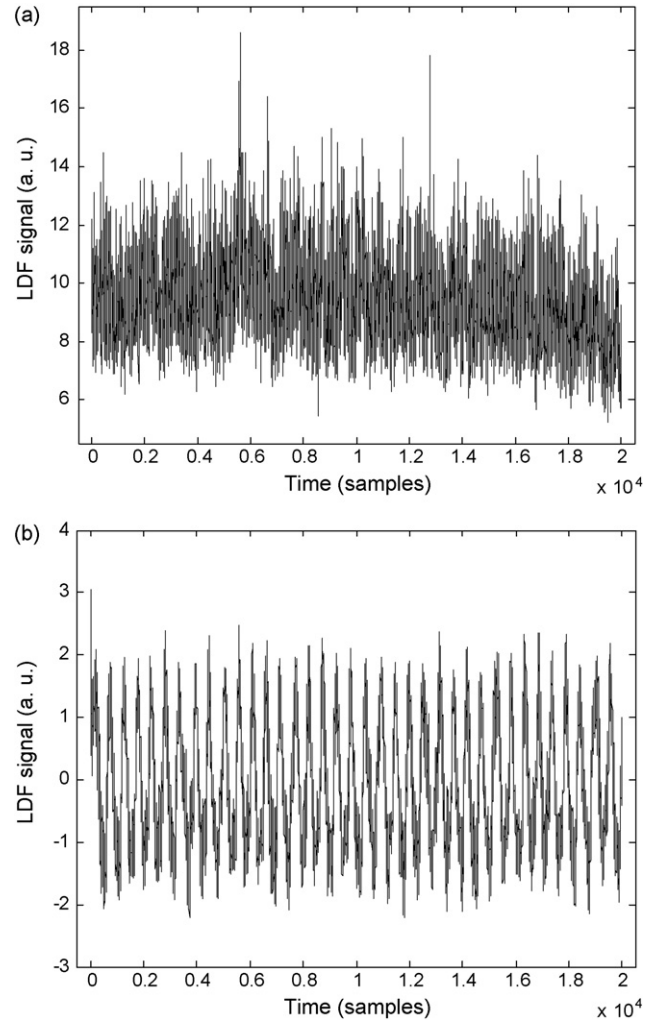

Fig. 1. a: experimental laser Doppler flowmetry (LDF) signal recorded in the forearm of a young healthy subject at rest (in arbitrary units); b: simulated signal based on six oscillators ($0.6 \times x_1 + 0.0002 \times x_2 + 0.6 \times x_3 + 0.2 \times x_4 + 0.6 \times x_5 + 0.5 \times x_6$) with linear and parametric couplings.

3. Multifractality analysis

Multifractals could be seen as a stretching of fractals. A multifractal signal is more complex than a (mono)fractal signal in the sense that it is always invariant by translation, although the dilatation factor needed to be able to discern the detail from the whole signal depends on the detail being observed. The multifractal analysis is so used to study signals, which have a local regularity that can vary from one point to another. The observation of the multifractility of such a signal is utilized in order to estimate his level of complexity. In our work, we use the parametric GQV based estimation method to estimate Hölder exponents of experimental and simulated LDF signals. Moreover, in what follows the method is first applied on a measure of white noise.

3.1. Hölder exponents

There are many ways to measure the local regularity of a signal. One of them, which has both strong theoretical bases and
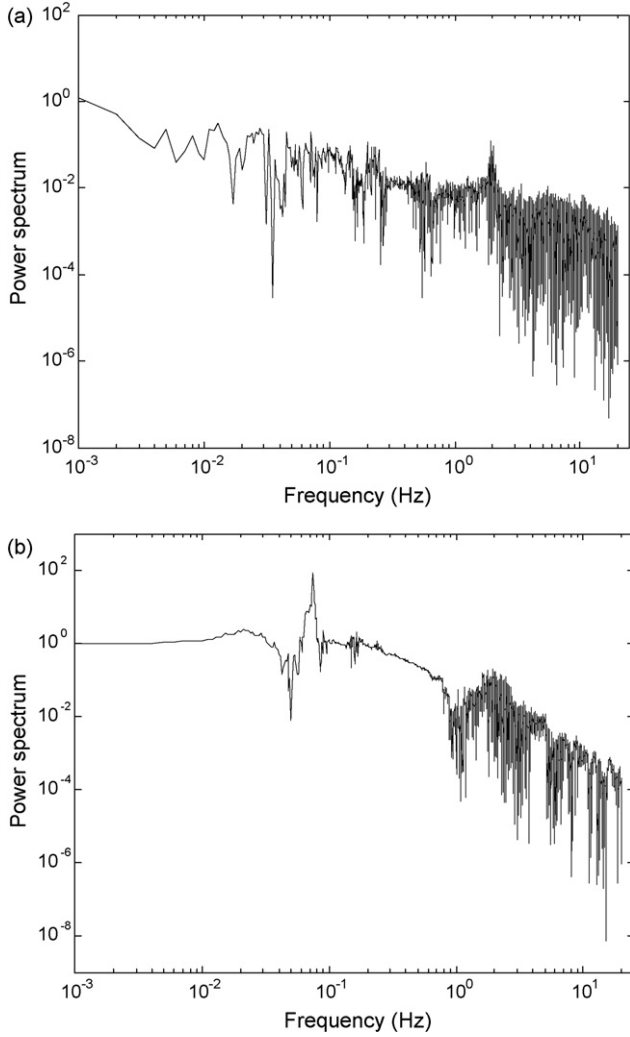
Fig. 2. a: power spectrum of an experimental laser Doppler flowmetry (LDF) signal recorded in the forearm of a young healthy subject at rest; b: power spectrum of a simulated signal based on six oscillators ($0.6 \times x_1 + 0.0002 \times x_2 + 0.6 \times x_3 + 0.2 \times x_4 + 0.6 \times x_5 + 0.5 \times x_6$) with linear and parametric couplings.

steady intuitive content, is the use of pointwise Hölder exponent [10]. For a positive measure represented by a signal $X(t)$, the Hölder exponent $\alpha(t_0)$ characterizes the strength of the singularity at $t = t_0$ [11]. When a "broad" range of exponents is found, signals are considered as multifractal. A "narrow" range implies monofractality. Multifractality in a process is a mark of a higher complexity compared to monofractal processes.

3.2. Generalised quadratic variation method

The parametric GQV based estimation method [12] is used to estimate Hölder exponents of signals. The algorithm is the following: with dimension d, for a trajectory $\tilde{B}\left(\frac{p}{N}\right)$ (sampled at the p/N moments, $P \in \{0, \ldots, N-1\}^d$) of a process, the quadratic

variations are defined by:

$$V_N = \sum_{p \,\in\, \{0,...,N-1\}^d} \left(\sum_{\varepsilon \,\in\, \{0,1\}^d} (-1)^{\varepsilon_1+...+\varepsilon_d} \tilde{B}\left(\frac{p+\varepsilon}{N}\right) \right)^2 \quad (6)$$

where $p = (p_1, ..., p_d)$, $\varepsilon = (\varepsilon_1, ..., \varepsilon_d)$ and $\frac{p+\varepsilon}{N} = \left(\frac{p_1+\varepsilon_1}{N}, \ldots, \frac{p_d+\varepsilon_d}{N}\right)$.

To obtain raises of the convergence speed for estimators according to the sampling step, the central limit theorem (CLT) is used. Some authors have shown that quadratic variations of a fBm with parameter H do not verify CLT for $H > 3/4$ [13]. That is why quadratic variations have been substituted by GQV [12]. For one dimensional multifractional Brownian motion (mBm), i.e. $d = 1$, the GQV gives [14]:

$$\tilde{V}_N(t) = \sum_{p \,\in\, \tilde{v}_N(t)} \left(\tilde{B}\left(\frac{p}{N^\delta}\right) - 2\tilde{B}\left(\frac{p+1}{N^\delta}\right) + \tilde{B}\left(\frac{p+2}{N^\delta}\right) \right)^2 \quad (7)$$

where $\tilde{v}_N(t) = \left\{ p \in N; 0 \leq p \leq N\text{-}2 \text{ and } \left| t\text{-}\frac{p}{N^\delta} \right| \leq N^{-\gamma} \right\}$ is the neighbourhood of t. γ and δ are two parameters, which modulate $\tilde{V}_N(t)$ such as $\delta - \gamma > 1/2$ and $\gamma \geq \delta \times b$ with $0 < b < 1$. It has been proven in [15] that for any mBm, under the technical assumptions on γ and δ, one has almost surely:

$$\lim_{N\to\infty} \frac{1}{2\delta} \left((1 - \gamma) - \frac{\log \tilde{V}_N(t)}{\log N} \right) = H(t) \quad (8)$$

It follows a simple algorithm to estimate the Hölder exponent $H(t_i)$ of a mBm $\tilde{B}$, sampled at the moments i/N, $i = 0, \ldots, N-1$ calculating first $\tilde{V}_N(t_i)$ for all $t_i = i/N$ then setting:

$$H(t_i) = \frac{1}{2\delta} \left((1 - \gamma) - \frac{\log \tilde{V}_N(t_i)}{\log N} \right) \quad (9)$$

We can rewrite (8) in the following form:

$$\log \tilde{V}_N(t_i) = \left[(1 - \gamma) - 2\delta H(t_i) \right] \log N \quad (10)$$

This method shows its weakness in the case of an mBm non-normalised. That is why we usually use a regression on N using the property of local autosimilarity of the mBm to get the slope $\alpha_1(.)$ such as:

$$\log \tilde{V}_N(t_i) = \alpha_1(t_i) \log N \quad (11)$$

By identification between (10) and (11) we get [14]:

$$H(t_i) = -\frac{\alpha_1(t_i) - (1 - \gamma)}{2\delta} \quad (12)$$

This method adds a lot of noise. To correct the latter, an adjustment has been proposed [14]:

$$\hat{H}_{\max\_reg} = \hat{H}_{\max} - \langle \hat{H}_{\max} \rangle + \langle \hat{H}_{reg} \rangle \quad (13)$$

where $\langle . \rangle$ is used for the temporal mean, i.e. for a numerical analysis, $\langle \hat{H} \rangle = \frac{1}{N} \sum_{i=0}^{N-1} \hat{H}(t_i)$. $\hat{H}_{\max}$ is the estimate obtained without regression and with $N = N_{\max}$, and $\hat{H}_{reg}$ is the estimate obtained with regression. Using the fact that the regression is not sensible

to the multiplicative factor, the idea is to keep just the temporal mean of this regression and to align the mean of $\hat{H}_{max}$ on this value. Good results have been obtained with this algorithm [14]. In our work, the parametric GQV method is carried out with the FracLab v2.0 tool [16].

3.3. Application of the GQV based estimation method on a measure of white noise

We first apply the parametric GQV based estimation method on a white noise measure as well as on its first and second order linearly filtered versions. In the continuous time domain, a first order linear low-pass filter, with time constant τ and a unity static gain, an input $x(t)$ and an output $y(t)$, has the following input-output differential equation:

$$\tau \frac{dy}{dt} = -y(t) + x(t) \tag{14}$$

We sample at the temporal step $\Delta t << \tau$ and use the Euler scheme for the numerical calculus of the derivative. Equation (14) becomes:

$$\tau \frac{y_{n+1} - y_n}{\Delta t} = -y_n + x_n \tag{15}$$

with $x_n = x(n\Delta t)$ and $y_n = y(n\Delta t)$. We deduce from (15) a numerical version of the first order linear low-pass filter, with time constant τ:

$$y_{n+1} = (1 - \frac{\Delta t}{\tau})y_n + \frac{\Delta t}{\tau}x_n \tag{16}$$

To realize a second order linear low-pass filter, we can cascade two first order filters.

White noises and their first order linearly filtered versions are known to be not differentiable (too irregular). We have to go up till a second order linear filter to obtain differentiable signals [17]. Hölder exponents lower than one mean that the corresponding signal is not differentiable. On the contrary, a signal with Hölder exponents higher than one is differentiable. These characteristics are therefore used herein in order to evaluate the parametric GQV based estimation method.

The results obtained with the parametric GQV based estimation method concerning a white noise realization and its filtered versions are qualitatively in accordance with the theory (see Fig. 3). From these first results, the parametric GQV based estimation method can be applied in its present form (FracLab v2.0 tool [15]) on experimental and simulated LDF signals.

4. Hölder exponents of laser Doppler flowmetry signals

We first estimate the Hölder exponents of the experimental LDF signals. To eliminate side effects we only take into account 18,000 Hölder exponents. For the example presented in Fig. 4, the Hölder exponents are between 0.42 and 0.57 (width of 0.15). Hölder exponents of our adjusted simulated signal (see Fig. 5) vary from 1.21 to 1.37 (width of 0.16). The average values obtained with all experimental LDF signals are shown in Table 1 and compared to those obtained with the simulated signal. Our work therefore shows that the range of Hölder
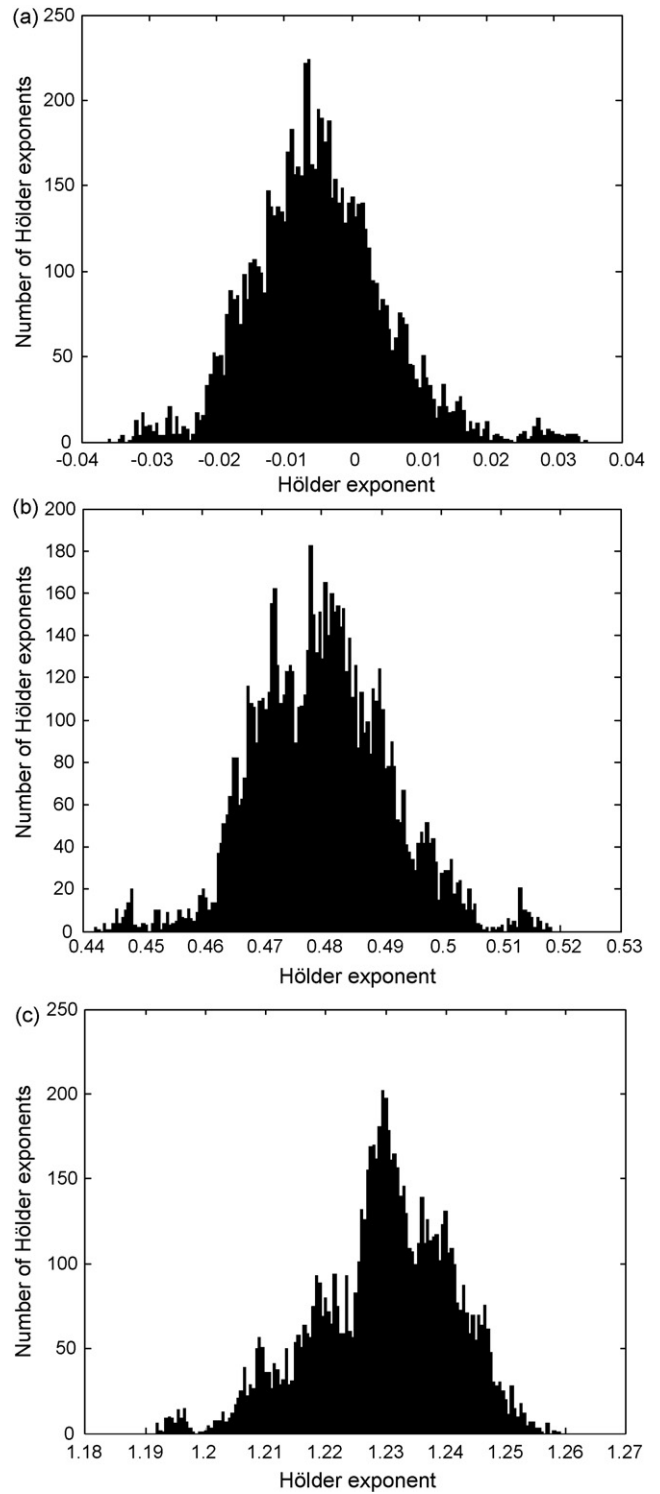

Fig. 3. Histogram of Hölder exponents, obtained with the parametric generalised quadratic variation (GQV) based estimation method for (a) a white noise measure, (b) its first order linear filtered version and (c) its second order linear filtered version.

exponents from experimental and simulated LDF signals are very similar. Furthermore, we can observe that contrary to the results obtained with the experimental data, the Hölder exponents estimated from the simulated signal are higher than one. The simulated signal is thus differentiable whereas the LDF sig-
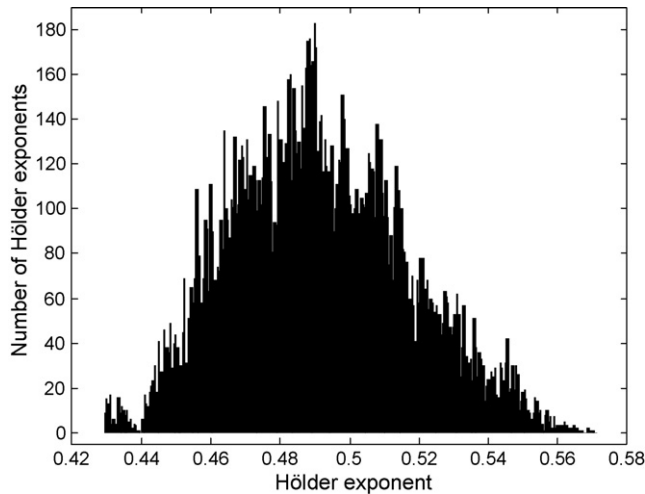
Fig. 4. Histogram of Hölder exponents, obtained with the parametric generalised quadratic variation (GQV) based estimation method for an experimental laser Doppler flowmetry (LDF) signal recorded in the forearm of a young healthy subject.
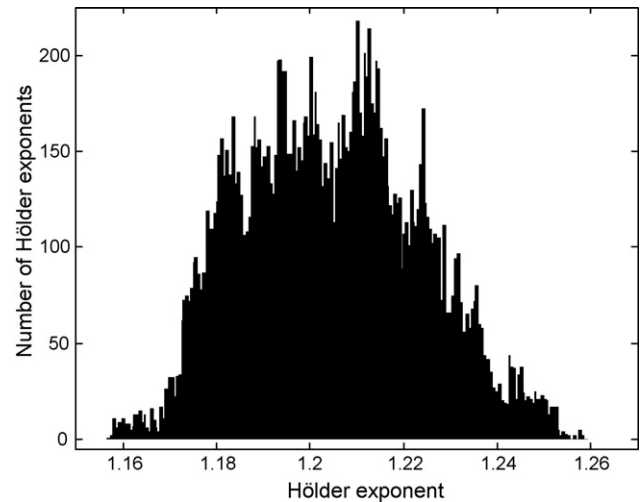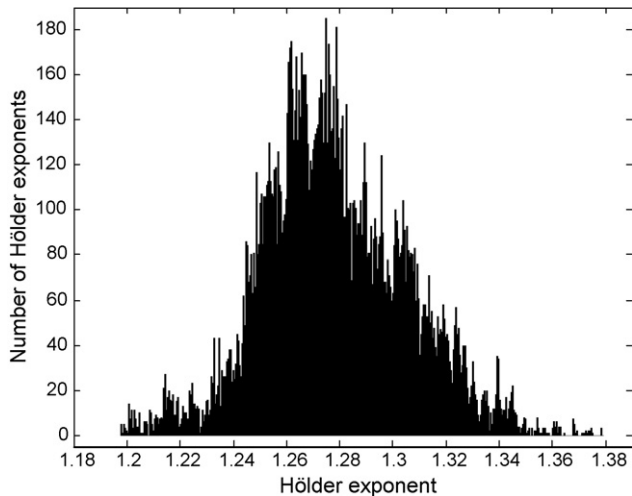

Fig. 5. Histogram of Hölder exponents, obtained with the parametric generalised quadratic variation (GQV) based estimation method for a simulated laser Doppler flowmetry (LDF) signal based on six oscillators with linear and parametric couplings.

nals recorded on the forearm of young healthy subjects are, on average, not differentiable.

Moreover, in order to understand how much complex are our LDF signals, we have compared the results obtained with a sig-

Table 1
Values of the Hölder exponents estimated for laser Doppler flowmetry (LDF) signals recorded in the forearm of healthy subjects (average value computed over seven subjects), for a simulated signal and for a monofractal signal (fractional Brownian motion [fBm]).

Signal	Minimal value	Maximal value	Range	Mean value	Standard deviation
Experimental LDF signals	0.76	0.92	0.15	0.84	0.02
Simulated LDF signal	1.21	1.37	0.16	1.27	0.02
fBm	0.46	0.53	0.07	0.49	0.01

Fig. 6. Histogram of Hölder exponents, obtained with the parametric generalised quadratic variation (GQV) based estimation method for an experimental laser Doppler flowmetry (LDF) signal recorded in the forearm of an elderly (59 years old) healthy subject.

nal having known properties (see Table 1), a fBm. The latter is a monofractal signal. We can thus observe that LDF signals (experimental and simulated) have a range for their Hölder exponents that is larger than the one obtained with an fBm. We can therefore consider that LDF signals recorded in the forearms of young healthy subjects can have weak multifractal properties. These results confirm those obtained in a recent study [2].

5. Conclusion

Our study confirms a weak multifractal behavior for peripheral blood flow signals recorded on the forearms of young healthy subjects at rest. It contributes to a quantitative assessment of the complexity of the data recorded from peripheral locations where intricate interactions at the microcirculation level take place. Moreover, on the one hand, the comparison between the values of the Hölder exponents of simulated and experimental signals leads to the conclusion that the model of six oscillators using linear and parametric couplings is adequate to reproduce the range of Hölder exponents observed in young healthy subjects. On the other hand, our results show that the model leads to differentiable signals contrary to the experimental LDF signals recorded in the forearm of young healthy people. Differentiable LDF signals are observed on elderly subjects (see an example in Fig. 6). A possible interpretation of these high values of Hölder exponents, proposed in [3], is a lower-quality information channel with a lot of redundancy for trustworthy transmission of information. However, the LDF signals recorded on elderly subjects have a narrowest range of Hölder exponents (see [3] and an example in Fig. 6) due to a loss of complexity. Therefore, this is a preliminary work since it is not able to exactly reproduce the multifractal behavior of experimental data.

This paper provides useful information to go deeper into the modeling of LDF data, and bring information for a better understanding of the peripheral cardiovascular system. The improvements, herein proposed for the model, have added com-

plexity (see [2]), as expected, but the simulated signal obtained has perhaps still too much redundancy information. Our results may therefore offer some guidelines for the construction of more adaptable models of LDF signals that could provide relevant physiological information. Further works are now needed in order to better understand the origin of the complexity of LDF signals (using for example methods based on the partition function) and to go deeper into the modeling. The observation of the influence of some pathology impacting the microvascular perfusion, like diabetes, on the multifractal behavior of LDF signals, could also be an interesting way of investigations.

Conflict of interest

None.

Acknowledgements

References

[1] Nilsson GE. Signal processor for laser Doppler tissue flowmeters. Med Biol Eng Comput 1984;22:343–8.

[2] Humeau A, Chapeau-Blondeau F, Rousseau D, Tartas M, Fromy B, Abraham P. Multifractality in the peripheral cardiovascular system from pointwise Hölder exponents of laser Doppler flowmetry signals. Biophys J 2007;93:L59–61.

[3] Humeau A, Chapeau-Blondeau F, Rousseau D, Trzepizur W, Abraham P. Multifractality, sample entropy, and wavelet analyses for age-related changes in the peripheral cardiovascular system: preliminary results. Med Phys 2008;35:717–23.

[4] Stefanovska A, Strle S, Bracic M, Haken H. Model synthesis of the coupled oscillators which regulate human blood flow dynamics. Nonlin Phenom Complex Syst 1999;22:72–87.

[5] Stefanosvka A, Bracic Lotric M, Strle S, Haken H. The cardiovascular system as coupled oscillators? Physiol Meas 2001;22:535–50.

[6] Stefanovska A, Luchinsky DG, McClintock PVE. Modelling couplings among the oscillators of the cardiovascular system. Physiol Meas 2001;22:551–64.

[7] Stefanovska A, Bracic M, Kvernmo HD. Wavelet analysis of oscillations in the peripheral blood circulation measured by laser Doppler technique. IEEE Trans Biomed Eng 1999;46:1230–9.

[8] Kvandal P, Landsverk SA, Bernjak A, Stefanovska A, Kvernmo HD, Kirkebøen K-A. Low-frequency oscillations of the laser Doppler perfusion signal in human skin. Microvasc Res 2006;72:120–7.

[9] Bračič M, Stefanovska A. Wavelet-based analysis of human blood-flow dynamics. Bull Math Biol 1998;60:919–35.

[10] Barriere O, Vehel JL. Local Hölder regularity-based modeling of RR intervals. CBMS 2008, 21th IEEE International Symposium on Computer-Based Medical Systems, 2008 June 17–19; Jyvaskyla, Finland.

[11] Struzik ZR. Determining local singularity strengths and their spectra with the wavelet transform. Fractals 2000;8(2):163–79.

[12] Istas J, Lang G. Quadratic variations and estimation of the local Hölder index of a Gaussian process. Ann Inst Henri Poincaré (B) Probabilités Stat 1997;33:407–36.

[13] Guyon X, Leon J. Convergence en loi des H-variations d'un processus Gaussien stationnaire sur R. Ann Inst Henri Poincaré (B) Probabilités Stat 1989;25:265–82.

[14] Barrière O. Synthèse et estimation de mouvements Browniens multifractionnaires et autres processus à régularité prescrite. Définition du processus auto régulé multifractionnaire et applications [thèse]. Nantes: école centrale de Nantes et université de Nantes; 2007, pp. 1–248.

[15] Ayache A, Lévy Véhel J. On the identification of the pointwise Hölder exponent of a generalized multifractional Brownian motion. Stochastic Process Appl 2004;111:119–56.

[16] Lévy Véhel J, Legrand P. Signal and Image processing with FracLab. FRACTAL04, Complexity and Fractals in Nature, 8th International Multidisciplinary Conference, 2004 April 4–7; Vancouver, Canada.

[17] Papoulis A. Probability, Random Variables, and Stochastic Processes. New York: McGraw-Hill; 1991.